Molecular Electronics

DOI: 10.1002/ange.201004899

Nitronyl Nitroxide Radicals as Organic Memory Elements with Both n- and p-Type Properties**

Junghyun Lee, Eunkyo Lee, Sangkwan Kim, Gyeong Sook Bang, David A. Shultz, Robert D. Schmidt, Malcolm D. E. Forbes, and Hyoyoung Lee**

Organic molecules are being actively explored for use in logical devices, either as individual memory elements or as components embedded in small organic and polymeric materials.[1] Conventional inorganic semiconductor devices are limited in terms of performance improvement owing to increased costs for device fabrication as well as physical limitations on minimum feature dimensions. Organic memory, however, is a possible substitute for both volatile and non-volatile memory devices. It has the advantages of facile tailoring through organic synthesis, simple device fabrication (even upon flexible substrates), and very low power consumption. Volatile organic memory is expected to be applied towards dynamic random access memory (DRAM), which typically requires a data refresh every few milliseconds, while non-volatile organic memory can be applied to read-only memory (ROM) and flash-type memory. Several types of organic and polymeric materials have been reported for this purpose, such as organic semiconductors,[2] charge-transfer complexes[3] (including redox-active compounds),[4] and metal-nanoparticle-dispersed thin films.[5] Recently, a new type of organic memory has been added to this list, namely organic radical molecules (nitroxide radicals, NO$^{\bullet}$) that contain an unpaired electron that is capable of undergoing oxidation or reduction by applied bias voltages.[6]

In 1901, Piloty and Schwerin succeeded in the synthesis and isolation of porphyrexide, the first organic nitroxide.[7] The most prominent member of this class of compounds is the 2,2,6,6-tetramethylpiperidine-*N*-oxyl radical (TEMPO).[8] TEMPO and many other NO radicals belong to the category of persistent radicals.[9] Since this pioneering work, the Nakahara group has reported the synthesis of a polymeric TEMPO radical derivative, poly(2,2,6,6-tetramethylpiperidinyloxy methacrylate) (PTMA), for an organic radical battery.[10] The research group of Nishide extended this work toward applications, such as radical batteries as cathode active materials,[11] organic light-emitting diodes as hole-injection layers,[12] and memory as p-type redox active materials.[6a] The TEMPO radical is easily oxidized to yield the corresponding oxoammonium salt, returning to the TEMPO radical by a p-type one-electron reduction.[13] However, for the complete circuit of the organic semiconducting device using PTMA, an n-type redox active material as a partner to the p-type material is required. Some previously reported polymer-based organic radical memory devices required additional organic layers, such as an electron-accepting layer for n-type[6a] and even a metal-particle-dispersed dielectric layer for actuation of the organic memory device.[6c] While previous research into polymer-based organic radical memory has led to significant advances, for a complete organic radical memory circuit it is crucial to find new organic radical molecules that demonstrate switchability and present both p- and n-type properties within the molecule. Also, new molecules can facilitate understanding of the origin of memory effects and whether that effect is induced by the organic radical alone or whether other environmental or chemical factors must be considered.

Herein we report novel molecular radical memory behavior using a stable organic radical molecule. We have synthesized and characterized the nitronyl nitroxide (NN) radical molecule 2-(3′-*tert*-butyl-4′,5′-dimethoxymethoxybiphenyl-4-yl)-4,4,5,5-tetramethylimidazolidine-1-oxyl-3-oxide (NN-Ph-CatMOM$_2$)[14] (see also the Supporting Information). The NN radical possesses one unpaired electron that is delocalized across the two equivalent N–O groups (Scheme 1).[15]

Owing to delocalization, the oxidized and reduced states of the NN radicals were expected to be stabilized over a wide window of applied voltages, leading to a high switchability for the NN radical memory. The ability of the NN-Ph-CatMOM$_2$ to act as both electron donor and acceptor was investigated by cyclic voltammetry (CV) and simultaneous electrochemical electron paramagnetic resonance (SEEPR) spectroscopy under an applied voltage.[16] Cyclic voltammograms were

[*] Dr. J. Lee, E. Lee, S. Kim, Dr. G. S. Bang, Prof. H. Lee
NCRI, Center for Smart Molecular Memory
Department of Chemistry, Sungkyunkwan University
Suwon 440-746 (Republic of Korea)
Fax: (+82) 31-299-5934
E-mail: hyoyoung@skku.edu
Prof. D. A. Shultz, Dr. R. D. Schmidt[+]
Department of Chemistry, North Carolina State University
Raleigh, NC 27695-8204 (USA)
Fax: (+1) 919-515-8920
E-mail: david_shultz@ncsu.edu
Prof. M. D. E. Forbes
Department of Chemistry
The University of North Carolina at Chapel Hill
Chapel Hill, NC 27599-3290 (USA)

[+] Present address: Department of Chemistry
The University of North Carolina at Chapel Hill
Chapel Hill, NC 27599-3290 (USA)

[**] This work was supported by the Creative Research Initiatives research fund (project title: Smart Molecular Memory) of MEST/NSF and the National Science Foundation (CHE-0943975).

Supporting information for this article is available on the WWW under http://dx.doi.org/10.1002/anie.201004899.

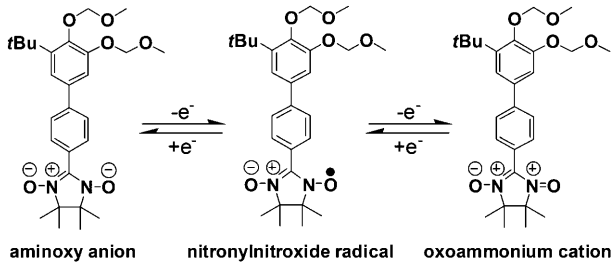

Scheme 1. Reversible redox mechanism of a NN-Ph-CatMOM$_2$ radical molecule.

obtained using an electrochemical analyzer and simultaneously recording the EPR spectra during the CV scan.[16] In general, the CV of the related NN radical compounds with an electron-donating group present a reversible redox couple at positive voltages, while NN radical compounds with an electron-withdrawing group showed a reversible redox couple at a negative voltage.[17] The CV of NN-Ph-CatMOM$_2$ is depicted in Figure 1.

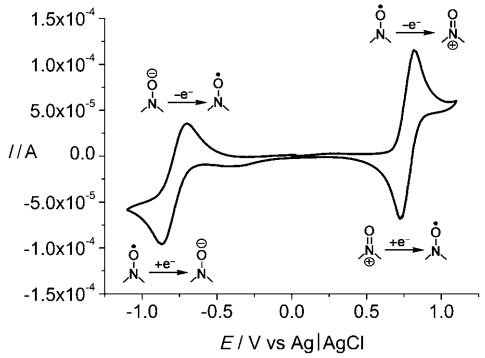

Figure 1. Cyclic voltammogram of a solution of 2.0 mM NN-Ph-CatMOM$_2$ in acetonitrile containing 0.1 M TBAPF$_6$ at a sweep rate of 0.1 V s^{-1} and using a glassy carbon electrode.

NN-Ph-CatMOM$_2$ displayed a reversible redox wave at 0.82 V versus Ag/AgCl, which was assigned to the corresponding NN/oxoammonium cation couple. This value was consistent with those observed in other nitroxides and NN radical compounds bearing electron-donating groups.[17] The redox reversibility could be ascribed to resonance delocalization of the oxoammonium cation. Importantly, NN-Ph-CatMOM$_2$ also exhibited a clear reversible redox wave at −0.74 V *vs* Ag/AgCl, which corresponds to the reduction of the NN radical to the corresponding aminoxy anion. This value was similar to nitroxide radical compounds having electron-withdrawing groups.[17] These redox waves were observed over more than 50 cycles without decomposition. The peak separation ($E_{pa}-E_{pc}$, with anodic peak potential E_{pa} and cathodic peak potential E_{pc}) for the anodic redox wave (positive region) of NN-Ph-CatMOM$_2$ was about 70 mV at scan rates of 100 mV s^{-1}. However, the peak separation in the cathode redox wave (negative region) was twice as wide (ca. 140 mV), while this value was narrower than that of the nitroxide compound reported in the literature.[17] This result suggests that NN-Ph-CatMOM$_2$ exhibits rapid heterogeneous electron-transfer kinetics.[18]

The SEEPR of the NN radical with zero applied potential (neutral state) consists of five lines ($g \approx 2.00$) in the ratio of 1:2:3:2:1 arising from the hyperfine coupling of two equivalent nitrogen atoms (nuclear spin $I = 1$) to the electron spin (Figure 2).[19] The SEEPR revealed a near complete disappearance of the strong EPR signal of NN-Ph-CatMOM$_2$ upon application of a +1.2 V potential (oxidized state). The EPR signal was regenerated upon returning the potential to +0.1 V (neutral state; Figure 2). This reversible redox couple was attributed to the oxidation of the NN radical to the oxoammonium cation of NN-Ph-CatMOM$_2$. Interestingly, the SEEPR signal for the NN-Ph-CatMOM$_2$ disappeared under an applied potential of −0.4 V (reduced state), which corresponded to the aminoxy anion, and was subsequently regenerated at −0.05 V (Figure 2). These results demonstrate the stabilization of the oxidized or reduced form of the NN radical. Thus, the redox-active organic NN radical possesses the necessary features for molecular memory controlled by an applied voltage. There was an appreciable formation of an impurity, iminonitroxide (IN) observed during the SEEPR experiments, as evidenced by the simulation in Figure 2 (light green hashed line, −0.05 V), which shows a mixture of about 58% NN and 42% IN.

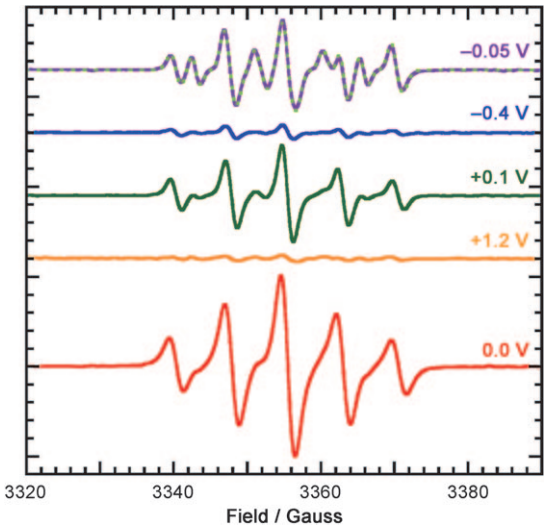

Figure 2. SEEPR of 98.1 μM NN-Ph-CatMOM$_2$ in *N*,*N*-dimethylformamide containing 100 mM TBAPF$_6$ using a gold helical electrode, measured versus a silver wire reference electrode.

A vertically structured metal–insulator–metal (MIM) diode for the fabricated organic radical memory is shown in Figure 3. The device is composed of a single layer of NN-Ph-CatMOM$_2$ molecules as the redox-active layer between two gold electrodes. Gold was selected for both electrodes, as it is known to have high oxidation resistance. This setup allows a clear demonstration of whether or not the origin of the memory effect comes from an intrinsic property of the NN radical molecule. The organic layer was spin-coated onto the bottom electrode from NN-Ph-CatMOM$_2$ dissolved in aceto-

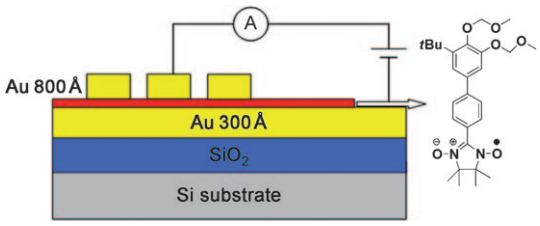

Figure 3. Cross-sectional view of the device layout for the NN-Ph-CatMOM$_2$ organic memory device.

nitrile. The thicknesses of the top and bottom electrodes were 80 and 30 nm, respectively. The thickness of the spin-coated radical film could be controlled from 17 to 100 nm, as measured by ellipsometry.

As we expected, the ON/OFF ratios sharply increased with an increase of radical film thickness. The ON/OFF ratios of the radical film were 2.5 (17 nm), 10 (35 nm), and 1000 (70 nm). As the film thickness increased, the OFF current sharply decreased, leading to an increased ON/OFF ratio. However, when the thickness of the radical film was over 100 nm, the *I*–*V* curve showed an insulating behavior. Furthermore, as the film thickness increased, threshold bias voltage for the ON current increased (Supporting Information, Figure S2). Figure 4 shows the *I*–*V* characteristics of the

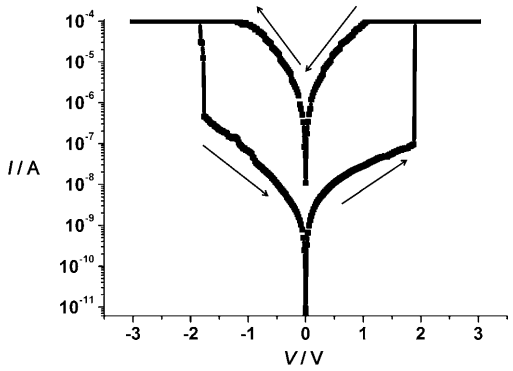

Figure 4. Hysteretic *I*–*V* characteristics of the molecular device (Au/NN-Ph-CatMOM$_2$/Au). The *I*–*V* characteristics of the devices were recorded by scanning the applied voltage from 0 to +3 V and then to −3 V, followed by a reverse scan from −3 to 0 V.

NN-Ph-CatMOM$_2$ with a thickness of about 70 nm. These curves were recorded by scanning the applied voltage initially from 0 to +3 V and then to −3 V, followed by a reverse scan from −3 to 0 V. The positive bias corresponds to a positive voltage applied to the top metal pad, whereas a negative bias corresponds to a negative voltage applied to the top pad. The *I*–*V* curves of NN-Ph-CatMOM$_2$ were symmetric, dipolar, stable, and reproducible for thousands of scans. As the positive bias voltage increased, the current starts to flow (OFF state) and suddenly increased at a threshold voltage of 1.9 V to a conductance state that is a positively charged oxoammonium cation (ON state). The conductive ON state was maintained even in the reverse sweep, ranging from 1.9 to −1.8 V, that is negatively charged aminoxy anion. Below −1.8 V, the device sharply switched to the OFF state. Surprisingly, despite the fact that some of NN-Ph-CatMOM$_2$ molecules were converted into IN-Ph-CatMOM$_2$ when returning back from the reduced to neutral state in the solution (Figure 2), the hysteresis of the solid state of the metal/NN-Ph-CatMOM$_2$/metal junction showed high reproducibility.

Stable conductivity switching behavior makes it possible for nonvolatile molecular memory phenomena to be tested under a voltage pulse sequence in a write–read–erase–read (WRER) cycle. In such a cycle, the high (write) and low (erase) conducting states were repeatedly induced and the read states monitored in between the high and low conducting states. A section of the voltage sequence and corresponding current from the device is shown in Figure 5. The device can be programmed to a high conductivity state using a +3.0 V

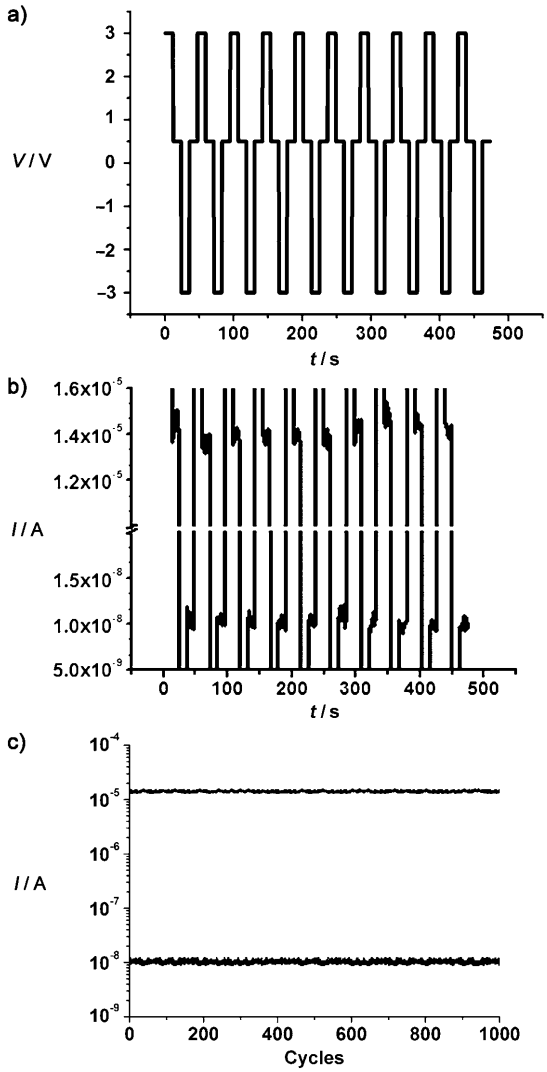

Figure 5. a) Input and b) output of write–read–erase–read (WRER) cycles of a molecular device containing NN-Ph-CatMOM$_2$ for rewritable data storage applications. Voltages: W +3.0, R 0.5, E −3.0, and R 0.5 V. c) Current in the ON and OFF states as a function of the number of WRER cycles. 1000 cycles were tested under vacuum.

pulse and to a low conductivity state using a −3.0 V pulse, with multiple current measurements for reading at +0.5 V. The WRER cycles can be repeatedly performed in an excess of 1000 cycles (Figure 5c). This device showed no significant degradation after several hundred WRER cycles. Figure 6

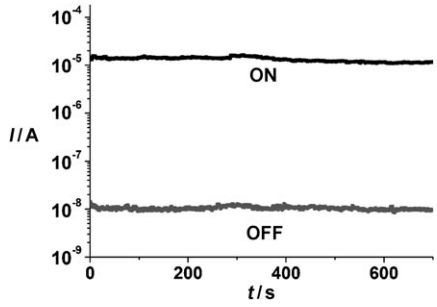

Figure 6. Retention times of the ON and OFF states of the NN-Ph-CatMOM$_2$ device, probed with voltages at 0.5 V. The ON and OFF states were induced by pulses of +3.0 and −3.0 V, respectively.

shows the typical retention time measured under inert conditions. Once the device is switched to the ON state by applying a positive voltage at +3.0 V, this state was retained after 700 s with no degradation. When the ON state was switched back to the OFF state by a negative voltage pulse applied at −3.0 V, the OFF state also was sustained.

In summary, cyclic voltammetry and SEEPR revealed that the NN radical molecule was a redox-active molecule with demonstrated switchability in both oxidized and reduced states. The organic NN radical device bearing a crossbar structure was easily fabricated by a wet process and showed both p- and n-type properties that functioned as a memory device. Based on the simple gold–molecule–gold device structure, we conclude that the origin of the switchability and memory phenomena of the NN radical memory device originated from the organic NN radical molecule, NN-Ph-CatMOM$_2$. The WRER cycles of the robust radical memory device showed no significant degradation after several hundred WRER cycles, even though only one radical thin layer was used. The transformation of NN to IN observed in solution cannot be directly related to degradation in the solid-state device. Such a transformation in the device would be manifest in an attenuation of current. However, as seen in Figure 5, the current is stable over at least 1000 cycles. This is the first known development of voltage-driven organic radical memory employing only one active layer of organic small molecules having both p- and n-type properties. Although the low ON–OFF ratio and switching cycles remained far from satisfactory in comparison with current silicon technology, our research on molecularly inherent radical memory provides new insight into the design of voltage-driven functional radical molecules.

Experimental Section

Organic solvents were freshly distilled from appropriate drying reagents prior to use. All starting materials were purchased from Aldrich and used without further purification. ^{1}H and ^{13}C NMR spectra were obtained on a Bruker Avance 400 spectrometer. NN-Ph-CatMOM$_2$ was prepared as described in the literature.[14] Cyclic voltammograms were obtained using a CHI 660 A electrochemical analyzer. An Ag(s) | AgCl(s) | KCl (satd) reference electrode and a platinum wire auxiliary electrode were used. All electrochemical measurements were carried out in a completely degassed solution. The thickness of the thin film was measured using a spectroscopic ellipsometer (Model J. A. Woollam VASE) at an incident angle of 60–70° and in a wavelength range between 200 and 1000 nm.

SEEPR experiments were conducted on a JEOL FA100 EPR spectrometer at the X-band (9.434 GHz) equipped with a JEOL helical electrolytic cell (JEOL ES-EL30) comprising a 5 mm diameter quartz tube, gold helical working electrode extending the length of the resonant cavity, gold auxiliary electrode insulated with Teflon and concentric to the helix, and a silver wire reference electrode. The applied bias was controlled with a Cypress Systems, Inc. Omni-101 microprocessor controlled potentiostat. Instrument parameters were kept constant and set to the following values: Center field 3360 G, sweep width ±40 G, 100 kHz modulation width 1 G, amplitude 1.6 × 100, time constant 0.3 s, scan time 2 min, one scan. A 98.1 μM solution of NN-Ph-CatMOM$_2$ was prepared in anhydrous *N*,*N*-dimethylformamide containing 100 mM TBAPF$_6$ (TBA = tetra-*n*-butylammonium). The sample solution (0.8 mL) was added to the electrolytic cell, the cell inserted into the resonant cavity, and the electrode leads attached to the potentiostat. The NN EPR signal was observed to decrease in intensity immediately under a positive (+1.2 V) applied bias. Returning to near neutral (+0.1 V) bias restored the NN signal, with the appearance of a small impurity. The signal was again decreased in intensity immediately under negative (−0.4 V) bias, and again returned to a near neutral (−0.05 V) bias, with significant growth of the impurity signal. The final spectrum (−0.05 V) was simulated using WinSim to obtain accurate hyperfine coupling constants (a_N).[20] This simulation shows the presence of two radical species: 58% nitronylnitroxide radical ($-a_N = 7.58$ G) and 42% iminonitroxide radical ($-a_{Na} = 9.29$ G and $a_{Nb} = 4.20$ G; see the Supporting Information, Figure S1).

Preparation of the Au/NN-Ph-CatMOM$_2$/Au device and characterization**:** Ti/Au metal with a thickness of 50 Å/300 Å was deposited onto a SiO$_2$/Si substrate by electron-beam evaporation. The surface roughness was approximately 5 Å (root-mean-square), as measured by atomic force microscopy (AFM) applied after a rapid thermal annealing process at 500°C for 30 s. Subsequently, the bottom electrodes were patterned with a line width of 60 μm using a stepper and a lift-off process. The bottom electrode was cleaned with piranha solution (98% H_2SO_4/30% H_2O_2 = 3:1 v/v) for 3 min. This was followed by washing several times with deionized water and ethanol and a final drying under a stream of nitrogen gas. For fabrication of the bulk organic memory device, NN-Ph-CatMOM$_2$ in acetonitrile solution was spun onto an gold substrate at 200 rpm for 10 s, followed by 1000 rpm for 30 s. The final speed was 2000 rpm for 10 s. The thin film was dried in a vacuum at room temperature overnight. A gold electrode (80 nm thick) was evaporated through a shadow mask onto a molecular layer using the electron beam evaporator under 5.0×10^{-7} Torr. SEM-EDS and DSC measurements were used to probe film formability and crystallinity (Supporting Information, Figures S3 and S4). The sample was tested in a variable-temperature probe station (Keithley 4200 semiconductor characterization system unit) under a vacuum of less than 10^{-3} Torr.

Received: August 6, 2010
Revised: February 5, 2011
Published online: April 7, 2011

Keywords: electron paramagnetic resonance · memory devices · molecular electronics · nitrogen radicals · organic radicals

[1] J. C. Scott, L. D. Bozano, *Adv. Mater.* **2007**, *19*, 1452.

[2] a) S. Möller, C. Perlov, W. Jackson, C. Taussig, S. R. Forrest, *Nature* **2003**, *426*, 166; b) D. Tondelier, K. Lmimouni, D. Vuilaume, *Appl. Phys. Lett.* **2004**, *85*, 5763; c) L. D. Bozano, B. W. Kean, V. R. Deline, J. R. Salem, J. C. Scott, *Appl. Phys. Lett.* **2004**, *84*, 607.

[3] a) R. S. Potember, T. O. Poehler, D. O. Cowan, *Appl. Phys. Lett.* **1979**, *34*, 405; b) T. Oyamada, H. Tanaka, K. Matsushige, H. Sasabe, C. Adachi, *Appl. Phys. Lett.* **2003**, *83*, 1252; c) Q. D. Ling, Y. Song, S. J. Ding, C. X. Zhu, D. S. H. Chan, D. L. Kwong, E. T. Kang, K. G. Neoh, *Adv. Mater.* **2005**, *17*, 455; d) Y. Song, Q. D. Ling, C. X. Zhu, E. T. Kang, D. S. H. Chan, Y. H. Sang, D. L. Kwong, *IEEE Electron Device Lett.* **2006**, *27*, 154; e) Q. D. Ling, Y. Song, S. L. Lim, E. Y. H. Teo, Y. P. Tan, C. X. Zhu, D. S. H. Chan, D. L. Kwong, E. T. Kang, K. G. Neoh, *Angew. Chem.* **2006**, *118*, 3013; *Angew. Chem. Int. Ed.* **2006**, *45*, 2947.

[4] a) Y. Gofer, H. Sarker, J. G. Killian, T. O Poehler, P. C. Searson, *Appl. Phys. Lett.* **1997**, *71*, 1582; b) K. Seo, A. V. Konchenko, J. Lee, G. S. Bang, H. Lee, *J. Am. Chem. Soc.* **2008**, *130*, 2553; c) J. Lee, H. Chang, S. Kim, G. S. Bang, H. Lee, *Angew. Chem.* **2009**, *121*, 8653; *Angew. Chem. Int. Ed.* **2009**, *48*, 8501.

[5] R. J. Tseng, J. Huang, J. Ouyang, R. B. Kaner, Y. Yang, *Nano Lett.* **2005**, *5*, 1077.

[6] a) Y. Yonekuta, T. Kurata, H. Nishide, *J. Photopolym. Sci. Technol.* **2005**, *18*, 39; b) Y. Yonekuta, K. Susuki, K. Oyaizu, K. Honda, H. Nishide, *J. Am. Chem. Soc.* **2007**, *129*, 14128; c) Y. Yonekuta, K. Honda, H. Nishide, *Polym. Adv. Technol.* **2008**, *19*, 281; d) K. Oyaizu, H. Nishide, *Adv. Mater.* **2009**, *21*, 2339.

[7] O. Piloty, B. Schwerin, *Chem. Ber.* **1901**, *34*, 2354.

[8] O. L. Lebedev, S. N. Kazarnovskii, *Tr. Khim. Khim. Tekhnol.* **1959**, *2*, 649.

[9] D. Griller, K. U. Ingold, *Acc. Chem. Res.* **1976**, *9*, 13.

[10] a) K. Nakahara, S. Iwasa, M. Satoh, Y. Morioka, J. Iriyama, M. Suguro, E. Hasegawa, *Chem. Phys. Lett.* **2002**, *359*, 351; b) H. Nishide, K. Oyaizu, *Science* **2008**, *319*, 737.

[11] H. Nishide, S. Iwasa, Y. J. Pu, T. Suga, K. Nakahara, M. Satoh, *Electrochim. Acta* **2004**, *50*, 827.

[12] T. Kurata, K. Koshika, F. Kato, J. Kido, H. Nishide, *Chem. Commun.* **2007**, 2986.

[13] P. Krzyczmonik, H. Scholl, *J. Electroanal. Chem.* **1992**, *335*, 233.

[14] D. A. Shultz, K. E. Vostrikova, S. H. Bodnar, H. J. Koo, M. H. Whangbo, M. L. Kirk, E. C. Depperman, J. W. Kampf, *J. Am. Chem. Soc.* **2003**, *125*, 1607.

[15] A. Caneschi, D. Gatteschi, R. Sessoli, *Acc. Chem. Res.* **1989**, *22*, 392.

[16] a) A. H. Maki, D. H. Geske, *J. Chem. Phys.* **1959**, *30*, 1356; b) D. H. Geske, A. H. Maki, *J. Am. Chem. Soc.* **1960**, *82*, 2671; c) I. B. Goldberg, A. J. Bard, *J. Phys. Chem.* **1971**, *75*, 3281; d) R. D. Allendoerfer, G. A. Martinchek, S. Bruckenstein, *Anal. Chem.* **1975**, *47*, 890.

[17] T. Suga, Y. J. Pu, S. Kasatori, H. Nishide, *Macromolecules* **2007**, *40*, 3167.

[18] T. Suga, Y. J. Pu, K. Oyaizu, H. Nishide, *Bull. Chem. Soc. Jpn.* **2004**, *77*, 2203.

[19] G. M. Rosen, S. Porasuphatana, P. Tsai, N. P. Ambulos, V. E. Galtsev, K. Ichikawa, H. J. Halpern, *Macromolecules* **2003**, *36*, 1021.

[20] D. R. Duling, *J. Magn. Reson. Ser. B* **1994**, *104*, 105.

